Lawrence Berkeley National Laboratory
LBL Publications

Title
Inverse Modeling of a Radial Multistep Outflow Experiment for Determining Unsaturated Hydraulic Properties

Permalink

Journal

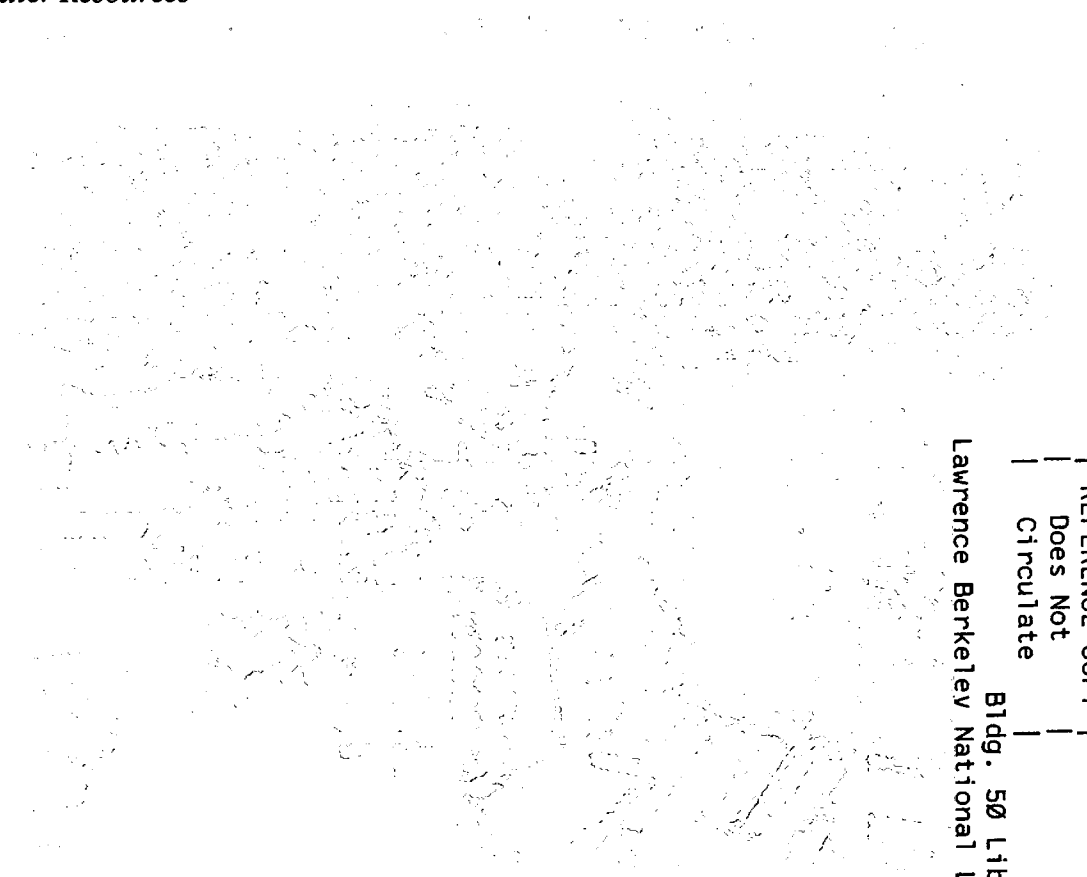**Author**
Finsterle, Stefan

Publication Date

ERNEST ORLANDO LAWRENCE
BERKELEY NATIONAL LABORATORY

Design and Analysis of an Experiment to Determine Hydraulic Parameters of Variably Saturated Porous Media

Stefan Finsterle and Boris Faybishenko
Earth Sciences Division

DISCLAIMER

Design and Analysis of an Experiment
to Determine Hydraulic Parameters
of Variably Saturated Porous Media

Stefan Finsterle and Boris Faybishenko

Lawrence Berkeley National Laboratory
Earth Sciences Division
University of California
Berkeley, CA 94720

DESIGN AND ANALYSIS OF AN EXPERIMENT TO DETERMINE HYDRAULIC PARAMETERS OF VARIABLY SATURATED POROUS MEDIA

Stefan Finsterle and Boris Faybishenko

Lawrence Berkeley National Laboratory, University of California, Berkeley

Abstract

Modeling flow and solute transport in the unsaturated zone on the basis of Richards equation requires specifying values for unsaturated hydraulic conductivity and water potential as a function of saturation. We developed experimental and analytical procedures that improve the determination of unsaturated hydraulic properties of soil samples. Numerical simulations, sensitivity analyses, and synthetic data inversions are used to assess the suitability of a proposed multi-step radial flow desaturation experiment. We calibrated different conceptual models against transient flow and pressure data from single-step and multi-step desaturation experiments to obtain estimates of absolute permeability as well as the parameters of the Brooks-Corey-Burdine and van Genuchten-Mualem relative permeability and capillary pressure functions. We discuss in detail the correlation structure of the parameters which is obtained from the error analysis. Furthermore, differences in the estimated parameter values illustrate the impact of the underlying model on the estimates. We conclude that the proposed radial desaturation experiment is suitable for the simultaneous determination of unsaturated hydraulic properties of a single soil sample, and that inverse modeling techniques provide the flexibility needed to analyze the data.

Introduction

Numerical models of transient water flow and contaminant transport in the vadose zone are usually based on the Richards equation, which requires knowledge about the unsaturated hydraulic conductivity and the water retention characteristics. The unsaturated hydraulic conductivity is a coefficient in Darcy's law modified for unsaturated flow. It describes the ability of a partially saturated porous medium to conduct fluid. Depending upon the variables used in Richards equation, the unsaturated hydraulic conductivity is expressed either as a function of pressure, hydraulic head, water content, or saturation. In this paper, we use the more general term effective permeability, defined as the product of the absolute permeability

k_{abs}, i.e., the permeability under quasi-saturated conditions, and the relative permeability $k_r(S)$, a dimensionless number between zero and one as a function of saturation S. The water retention curve describes the capillary pressure $p_c(S)$ as a function of saturation. It is also a measure of the water capacity of the soil.

There are several different approaches to the determination of unsaturated hydraulic properties. Capillary pressure curves can be constructed pointwise by directly measuring saturation and water potentials under equilibrium conditions. For use in numerical models, a functional form has to be selected representing the experimental data. These parametric models can be considered mere fitting functions. However, they contain parameters that are representative of the pore structure. An example is the λ parameter of the Brooks-Corey model [*Brooks and Corey*, 1964] which can be related to the pore size distribution or fractal dimension of the pore space [*Perfect et al.*, 1996]. Texture and other easily measured soil properties have also been used to estimate parameters of a closed-form functional expression [*Saxton et al.*, 1986; *Rawls and Brakensiek*, 1989]. These methods infer the characteristic curves using limited data and a model of the pore space. A similar approach is applied when predicting unsaturated hydraulic conductivity from water retention curves. Standard pore connectivity models relating capillary pressure and relative permeability functions were introduced by *Burdine* [1953] and *Mualem* [1976], and are used in the expressions of *Brooks and Corey* [1964] and *van Genuchten* [1980], respectively.

In the indirect approach, parameters of closed-form expressions are estimated by inverse modeling by matching the solutions of the Richards equation to observed data. While the approaches discussed above rely on direct observations or make use of purely mathematical or geometric models, inverse modeling involves process simulation, i.e., it uses the equations governing flow in unsaturated porous media. In inverse modeling, any type of data can be used for parameter estimation, provided that the calculated system response is sensitive to the parameters of interest. This method will be discussed in greater detail below.

A large number of laboratory and field methods have been developed to determine unsaturated hydraulic properties of soils [*Gardner*, 1956; *Kool et al.*, 1985]. The conventional methods are usually time-consuming and expensive. Moreover, they do not permit the determination of both relative permeability and capillary pressure curves during a single experiment, which often leads to inconsistent parameters and thus unreliable model predictions [*Luckner et al.*, 1989; *Clausnitzer et al.*, 1992]. The disadvantages of the traditional methods have been discussed by *Salehzadeh and Demond* [1994]. They also reviewed recent measurement techniques and designed a laboratory apparatus for rapid and simultaneous measurement of capillary pressure and relative permeability functions.

As previously mentioned, numerical simulation and inversion techniques impose few restrictions on the experimental layout. Unlike analytical methods, inverse modeling does not require specific flow geometries and boundary conditions. Any type of sensitive observation, for which a corresponding model result can be calculated, is suitable for parameter estimation. Prior to testing, design calculations can be conducted by means of synthetic data inversions. Performing synthetic inversions reduces the risk of producing an ill-posed inverse problem when analyzing the actual data. Transient data of different types, such as pressure and flow rate measurements, can be inverted simultaneously, constraining the solution of the inverse problem. A formalized residual and error analysis provides additional insight into the system behavior and the estimated parameter set.

Solving the inverse problem is usually defined as the estimation of parameters by calibrating a model against the observed data. In the broader sense of model identification, however, inverse modeling also requires identifying the most suitable conceptual model. The main advantage of analyzing laboratory data is that flow geometry as well as initial and boundary conditions are usually well defined. Nevertheless, a major part of the conceptual model to be identified is the parametric form describing relative permeability and capillary pressure as a function of saturation. Once the functional form is selected, the parameters of the model can be determined. Because the parameter estimates strictly refer to and are only optimal for the given model structure, choosing the most likely conceptual model is essential. Therefore, test design should include a criterion that evaluates the capability of a proposed experiment to produce selective data with respect to the conceptual model. These ideas have been developed and refined in papers by *Knopman and Voss* [1988, 1989], *Knopman et al.* [1991], and *Finsterle and Pruess* [1996].

A number of inverse modeling techniques for the determination of unsaturated hydraulic properties from single-step and multi-step radial flow experiments have been discussed in the literature [*Kool et al.*, 1989; *Simunek and van Genuchten*, 1996]. In this study, we utilize the multi-phase flow simulator TOUGH2 [*Pruess*, 1991] and optimization model ITOUGH2 [*Finsterle*, 1997]; they have been described in detail in *Finsterle and Pruess* [1995].

The main purpose of this paper is to evaluate experimental procedures using inverse modeling techniques. The objective is to optimize the design of an experiment for the determination of unsaturated hydraulic properties. Measurements were carried out on undisturbed loamy soil cores [*Dzekunov et al.*, 1987], and analyzed by inverse modeling.

We first address the design of a radial, single-core experiment, followed by a formal assessment of parameter identifiability. Finally an application of inverse modeling to the actual data is presented.
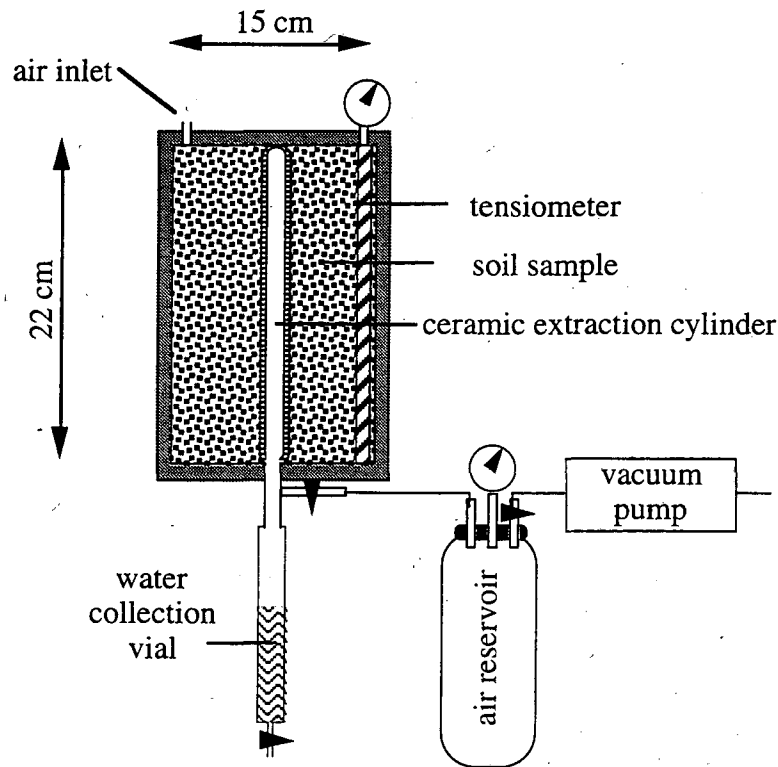
Radial Flow Experiment

We first describe a laboratory setup for a single- and multi-step radial desaturation experiment. Experiments with a radial flow geometry were first described by *Gardner* [1956]. The technique was tested and substantially improved by *Faybishenko* [1986] and *Dzekunov et al.* [1987] who performed experiments using different designs of the central porous cylinder for both injection and extraction, and variable locations of the monitoring tensiometers. They conducted wetting and drying experiments by applying single-step, multi-step, and continuously changing boundary pressures under isothermal and non-isothermal conditions.

Figure 1 shows a schematic of a flow cell apparatus for radial desaturation experiments on soil samples. The central extraction cylinder is eliminates uncontrolled water exchange between the soil and the cylinder as a result of air diffusion through the ceramic cup.

The experimental procedure can be described as follows. Soil cores (22 cm long and 15-18 cm in diameter) are cut in the field using a special cylindrical knife which minimizes the disturbance of the sample [*Faybishenko*, 1986; *Dzekunov et al.*, 1987]. The cores are conserved in a solid metal or plastic cylinder. In the laboratory, a hole with a diameter of 2.3 cm is drilled coaxially at the center of the core, in which a ceramic cylinder is inserted with an air entry pressure of about 1 bar.

The samples are then fully saturated under vacuum, thus reducing the effects of entrapped air on the determination of unsaturated hydraulic parameters. Note, however, that air is introduced and may be entrapped during the subsequent drying of the core.

The apparatus is instrumented with a vial to measure the cumulative water discharge through the central porous cylinder, and a tensiometer for water potential measurements within the soil sample.

15 cm

air inlet

tensiometer

soil sample

ceramic extraction cylinder

22 cm

vacuum pump

water collection vial

air reservoir

Figure 1. Schematic of apparatus for radial flow experiment to determine unsaturated hydraulic properties.

Numerical Simulation of Multi-Step Desaturation Experiment

In this section, we discuss numerical simulations of a multi-step, radial flow experiment, and assess the suitability of the design described above for the estimation of unsaturated hydraulic properties. A number of criteria have been proposed to measure the performance of an experimental design (see, for example, *Steinberg and Hunter* [1984], *Knopman and Voss* [1988; 1989], *Sun and Yeh* [1990], *Finsterle and Pruess* [1996]). The experiment should provide sufficiently sensitive data so that the parameters can be determined with an acceptably low estimation uncertainty. Furthermore, it should be possible to formulate a well-posed inverse problem, leading to unique and stable solutions.

The suitability of an experimental setup for parameter estimation can be examined prior to data acquisition. Design calculations provide insight into the sensitivity of each potential observation with respect to the parameters, and synthetic model calibrations can be performed to assess the solution of the inverse problem. As an example, we model a synthetic multi-

step desaturation experiment where the suction pressure at the center of a cylindrical core is reduced in discrete steps from -2 kPa to -10, -20, -30, -60, and -90 kPa after 1, 2, 3, 5, and 10 days, respectively. It is assumed that the cumulative outflow is recorded as a function of time, and that a tensiometer is installed for capillary pressure measurements. The standard deviation of the outflow and pressure measurement error is assumed to be 10 ml and 2 kPa, respectively.

Design calculations must be based on preliminary information about the system, and a conceptual model of the experiment should mimic the expected conditions. A crucial part of the conceptual model is the choice of the characteristic curves. In the simulations discussed in this section, we use the Brooks-Corey-Burdine (BCB) model [*Brooks and Corey*, 1964; *Burdine*, 1953] to describe the capillary pressure and relative liquid permeability as a function of liquid saturation S_l:

$$p_c = -p_e \cdot S_e^{-\frac{1}{\lambda}} \tag{1}$$

$$k_r = S_e^{\frac{2+3\lambda}{\lambda}} \tag{2}$$

Here, p_e and λ are fitting parameters sometimes referred to as air entry pressure and pore size distribution index, respectively. The effective liquid saturation S_e is defined as

$$S_e = \frac{S_l - S_{lr}}{1 - S_{lr}} \tag{3}$$

where S_{lr} is the residual liquid saturation.

The performance of the proposed radial flow experiment is analyzed assuming that three parameters are to be estimated based on capillary pressure and cumulative outflow data. The three parameters are the logarithm of the absolute permeability, $\log(k_{abs})$, the pore size distribution index, λ, and the logarithm of the air entry pressure, $\log(p_e)$.

Figure 2 shows the simulated system behavior for the conceptual model and base case parameter set given in Table 1. The outflow and capillary pressure curves represent potential data to be used in an inversion for the determination of the three parameters of interest. While the pressure prescribed at the central extraction cylinder is reduced in discrete steps, the capillary pressure at the outer wall of the flow cell decreases rather smoothly. The cumulative outflow through the extraction cylinder reaches 900 ml at the end of the experiment, draining the sample to about 50 % of the initial water content.
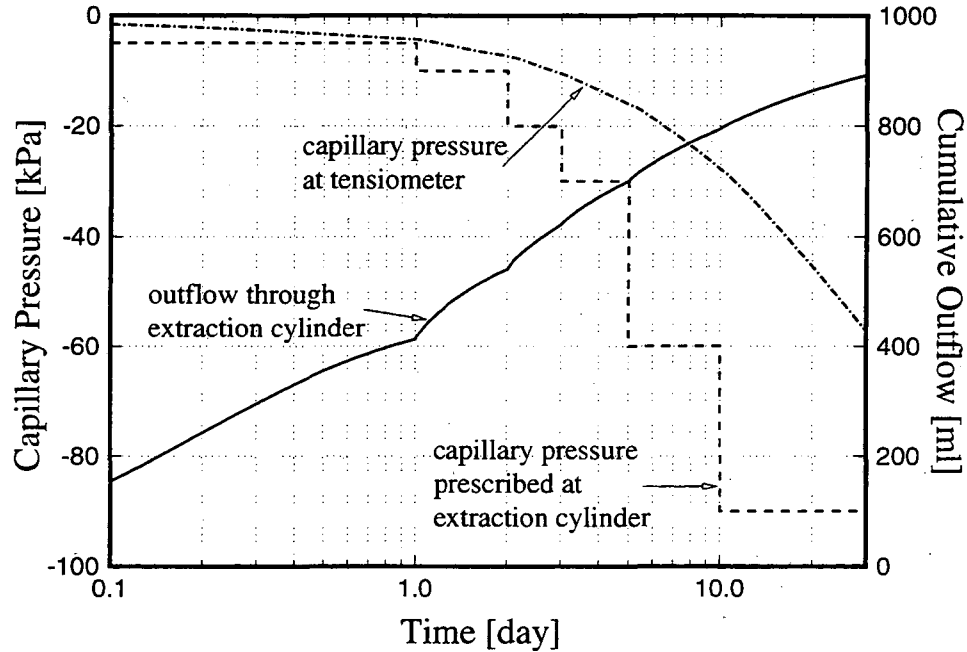
Figure 2. Simulated cumulative outflow through central extraction cylinder and capillary pressure near wall of flow cell. The total pore volume is 1820 ml.

Table 1. Base Case Parameter Set and Expected Parameter Variation

Parameter	Base Case Value	σ_p
$\log(k_{abs}$ [m^2])	-13.00	1.00
pore size distribution index λ	0.25	0.25
$\log(p_e$ [Pa])	3.00	0.50

We first perform a sensitivity analysis to determine the optimal location of the tensiometer. As a general rule, the location within the core sample yielding the maximum total sensitivity provides the most information about the model parameters to be estimated. Note that relying on a sensitivity analysis for experimental design does not address the question whether the parameters of interest can be determined independently. High sensitivity is only a necessary, but not sufficient condition for a well-posed inverse problem (for a detailed discussion of this point see *Finsterle and Persoff* [1996]).

The dimensionless sensitivity measure consists of a sum of the absolute values of the sensitivity coefficients $\partial z_i/\partial p_j$, scaled by the measurement error σ_{z_i} and the expected parameter variation σ_{p_j}:

$$\Omega_j = \sum_{i=1}^{M} \left| \frac{\partial z_i}{\partial p_j} \cdot \frac{\sigma_{p_j}}{\sigma_{z_i}} \right| \qquad (4)$$

Here, z_i indicates any type of observable variable, where M is the total number of calibration points in space and time, and p_j is the parameter to be estimated. The scaling of the sensitivity coefficients is necessary to compare the contribution of different data types to the solution of the inverse problem, and to evaluate the sensitivity of parameters that vary over different scales depending on their measurement units and physical nature.

Simulations were performed using the parameter set in Table 1, and the sensitivity measure (4) was evaluated for different potential locations of the monitoring tensiometer. The dependence of sensitivity on sensor location results from the lack of capillary equilibrium during the transient phase of the experiment. Figure 3 shows the sensitivity measure as a function of radial distance of the tensiometer from the core axis. Recall that a capillary pressure boundary condition is prescribed at the ceramic cylinder in the center of the core. Consequently, the capillary pressure near the axis of the core is not sensitive to changes in the parameters. Optimal data sensitivity is reached if the tensiometer is placed at a radial distance of about 0.028 m from the extraction cylinder. Note, however, that the decline of the curve with increasing distance is very weak as a result of the high permeability and the finite volume of the core. Because of the non-linearity of unsaturated flow problems, the curves shown in Figure 3 depend on the base case parameter set, i.e., the point of maximum sensitivity may shift considerably if soil conditions vary. For example, if the permeability of the sample is higher than expected, the zone of low sensitivity around the core axis is larger. While an optimum design prefers a tensiometer relatively close to the center of the core, a robust design suggests installation near the outer wall of the flow cell to avoid the low sensitivity zone in the case of higher permeability. If permeability happens to be lower than expected, the sensitivity at the outer boundary decreases slightly, but remains acceptable.

Figure 4 shows the scaled sensitivity coefficients of the cumulative outflow with respect to $\log(k_{abs})$, λ, and $\log(p_e)$, plotted as a function of time. Extrapolating the initial trend, the sensitivity of λ and $\log(p_e)$ increase continuously with time. One might conclude from this that both parameters can be precisely determined at equilibrium. However, the parameters would be determined based solely on the saturation condition at equilibrium. This has two disadvantages. First, a potential measurement error in the equilibrium data point is not controlled by other measurements. Therefore, it has a direct influence on the estimates; the inverse problem is unstable. Second, it is preferable to obtain an optimum parameter set that represents the average behavior over the entire range of saturation. If too many late-time

data are used for the inversion, the result will be biased towards the conditions at low saturation near steady state. The problem of overbalanced late-time data can be partly alleviated by introducing a measurement standard deviation that increases with the cumulative amount of liquid extracted. The bias can also be overcome by performing a multi-step desaturation experiment, where data is collected at different capillary pressure and saturation levels. If performing a joint inversion of all transient data as proposed here, a new step should be invoked so that a nearly constant total sensitivity is maintained, as shown in Figure 4. Also note that the sensitivity of $\log(k_{abs})$ decreases when flow rates become small towards the end of a step. It is important to maintain a balance between the sensitivity of $\log(k_{abs})$ and the BCB parameters to avoid a permeability estimate that is governed by its correlation to λ and $\log(p_e)$.

We have illustrated the use and limitations of a sensitivity analysis for experimental design and the difference between an optimal and robust design. Additional design criteria are discussed in the following section.
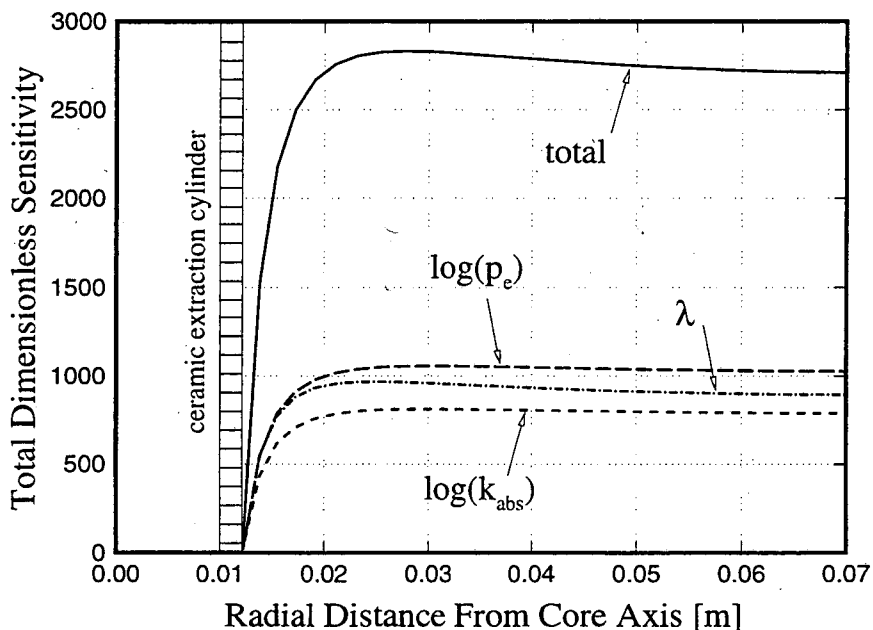
Figure 3. Dimensionless sensitivity of capillary pressure summed over time with respect to $\log(k_{abs})$, λ, and $\log(p_e)$ as a function of tensiometer location. A time-varying suction pressure is prescribed at the extraction cylinder.
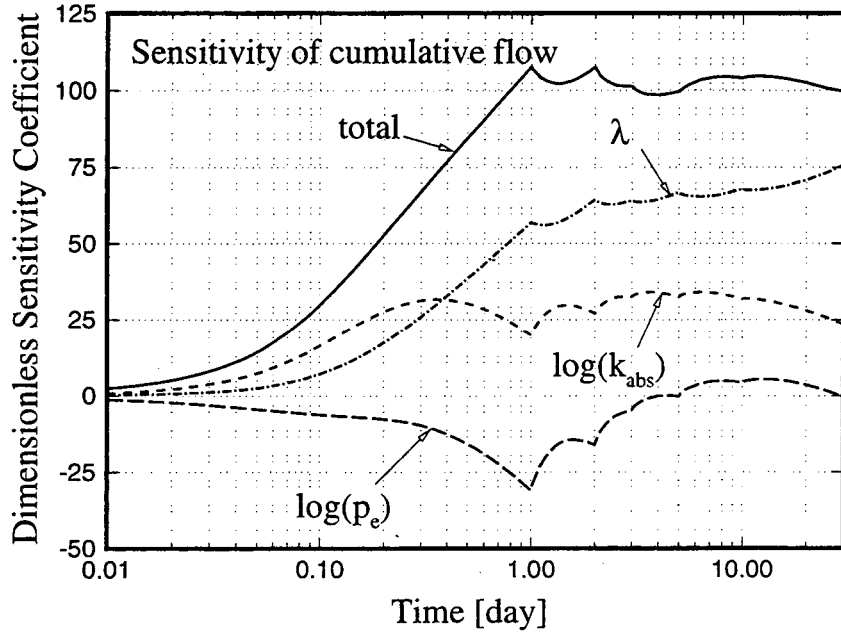
Figure 4. Dimensionless sensitivity coefficient of cumulative outflow with respect to $\log(k_{abs})$, λ, and $\log(p_e)$ as a function of time.

Well-Posedness of Inverse Problem

As indicated in the previous section, strong correlations among the parameters may severely affect the quality of the inverse modeling results if random or systematic errors are present. Because parameter correlations are not addressed by a standard sensitivity analysis, design calculations should also include synthetic data inversions to examine the potential estimation uncertainty and correlation structure. The design should then be optimized to minimize the trace or determinant of the resulting covariance matrix [*Steinberg and Hunter*, 1984; *Finsterle and Pruess*, 1996].

Contouring the objective function S, given by

$$S = \mathbf{r}^T \mathbf{C}_{zz}^{-1} \mathbf{r} \tag{5}$$

is a means to visualize the well- or ill-posedness of the inverse problem. In (5), $\mathbf{r}$ is the vector of residuals comprised of the differences between the observed and calculated system response, and $\mathbf{C}_{zz}$ is the observation covariance matrix. Points of equal value of the objective function lie on continuous surfaces in the three-dimensional parameter space

$\log(k_{abs})$, λ, and $\log(p_e)$. Figure 5 shows contour plots in the three parameter planes $\log(k_{abs})$-$\log(p_e)$, $\log(k_{abs})$-λ, and λ-$\log(p_e)$, intersecting the minimum. The shape, size, orientation, and convexity of the minimum provides information about the uniqueness and stability of the inversion, and represents the uncertainty and correlation structure of the estimated parameter set. Furthermore, the presence of local minima can be detected readily. It should be realized, however, that Figure 5 examines only a subregion of the parameter space, and that the algorithm employed for automatic parameter estimation relies on the local examination of the objective function to identify its minimum and the curvature at the solution.

Information about the structure of the objective function can be obtained from an analysis of the covariance matrix. We will discuss these issues later for the actual inversion of laboratory data rather than in the context of numerical design calculations.
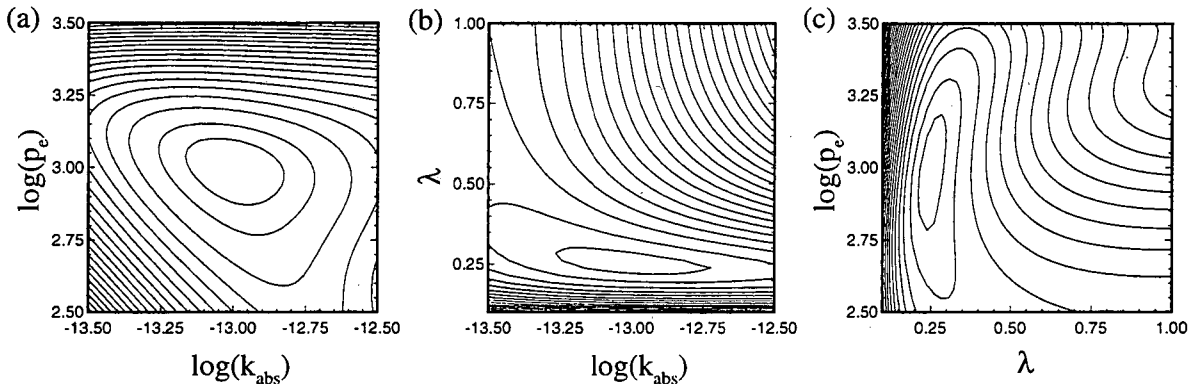
Figure 5. Contours of the objective function in the three parameter planes (a) $\log(k_{abs})$-$\log(p_e)$, (b) $\log(k_{abs})$-λ, and (c) λ-$\log(p_e)$. The planes intersect the parameter space at the global minimum, i.e., they contain the best estimate parameter set.

In the absence of measurement errors, the objective function visualized in Figure 5 is devoid of local minima. Synthetic inversions demonstrate that the global minimum, which is known, is accurately identified by the Levenberg-Marquardt minimization algorithm. The covariance/correlation matrix calculated at the minimum indicates that it should be feasible to obtain accurate parameter estimates using the proposed multi-step desaturation experiment. This conclusion is based on the assumption that the standard deviations of the final flow and pressure residuals is not larger than 25 ml (i.e., about 1.5 % of the total pore volume) and 5 kPa, respectively.

Inversion of Experimental Data

We analyze radial desaturation experiments performed on a soil of clay loam with a dry density of about 1.5 g/cm^3, a clay content of 30 %, and a porosity of 0.48. Two data sets are analyzed, one from a single-step and one from a multi-step experiment, and two different conceptual models are used to match the data. The first set of cumulative outflow and capillary pressure data are obtained from a single-step experiment with an applied suction pressure at the extraction cylinder of -98 kPa. The second experiment is a multi-step experiment similar to the one described above. The sequence of applied suction pressures was chosen such that the data allow for a pointwise construction of the water retention curve for comparison with inverse modeling results (see discussion of Figure 10 below). In this experiment, the applied suction pressure is temporarily increased as shown in Figure 8 below, allowing water to redistribute within the core.

Inverse modeling was used to analyze the data from the two radial flow experiments. Following the proposed test design, the cumulative water discharge through the ceramic extraction cylinder and the water potential near the outer wall of the flow cell are used to estimate permeability, pore size distribution index, and air entry pressure.

As mentioned earlier, the estimated parameter values will depend on the functional model used to describe capillary pressure and relative permeability of the soil. The estimate of absolute permeability is influenced by the choice of the characteristic curves because permeability is concurrently determined and thus correlated to the parameters of the capillary pressure and relative permeability function. Therefore, it is crucial to identify the functional model that best represents the true conditions. As an alternative to the BCB model (see Equ. (1) - (3)), the data were also analyzed using the van Genuchten-Mualem model (VGM) [*van Genuchten*, 1980]:

$$p_c = -\frac{1}{\alpha}\left(S_e^{-1/m} - 1\right)^{1/n}$$

(6)

$$k_r = S_e^{1/2}\left[1 - \left(1 - S_e^{1/m}\right)^m\right]^2$$

(7)

where

$$m = 1 - \frac{1}{n}$$

(8)

For convenience and based on a weak analogy to the BCB model described by *Morel-Seytoux et al.* [1996], we will refer to parameter n as the pore size distribution index, and

$1/\alpha$ as the air entry pressure. While the two models, BCB and VGM, exhibit only minor differences in the capillary pressure function for intermediate and low liquid saturations, the system behavior may differ near full saturation. For example, the prediction of the initial amount of water drained from a fully liquid-saturated core under small capillary suction depends on the shape of the capillary pressure and relative permeability curves at high saturation, a function of the volume and distribution of the larger pores [*Luthin*, 1957]. Because cumulative outflow data contain a contribution from the drainage of the larger pores, the two models are expected to perform differently when calibrated against the observed outflow and capillary pressure measurements.

The model is calibrated by minimizing the weighted least-squares objective function (Eq. 5) using the Levenberg-Marquardt algorithm [*Beck and Arnold*, 1977].

Figure 6 shows contour plots of the objective function in three orthogonal parameter planes through the minimum for the multi-step experiment using the BCB model. The minimum exhibits similar characteristics to that constructed with the synthetic data during the design stage of the experiment (see Figure 5). Also depicted are the projections of the solution path taken by the Levenberg-Marquardt minimization algorithm. The minimum is accurately identified within five iterations.
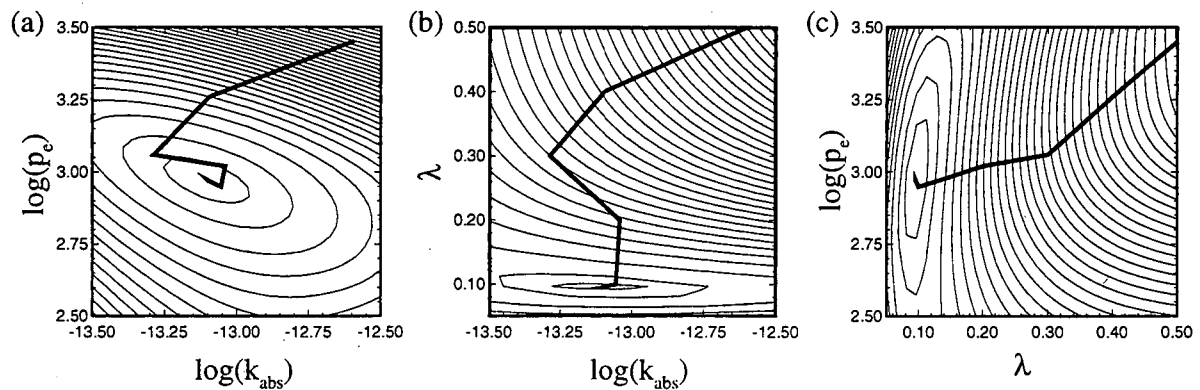
Figure 6. Contours of the objective function in the three parameter planes (a) $\log(k_{abs})$-$\log(p_e)$, (b) $\log(k_{abs})$-λ, and (c) λ-$\log(p_e)$. The projections of the solution path taken by the Levenberg-Marquardt minimization algorithm is shown as a bold line.

The BCB and the VGM model are calibrated against the outflow and pressure data from the single-step and multi-step experiment. The results of the four inversions are compared with regard to the estimated parameters, the goodness-of-fit achieved, estimation uncertainty,

and overall parameter correlation. The goodness-of-fit is measured by the estimated error variance s_0^2:

$$s_0^2 = \frac{\mathbf{r}^T \mathbf{C}_{zz}^{-1} \mathbf{r}}{M - N} \tag{9}$$

Here, M is the number of observations, and N is the number of parameters. The smaller s_0^2, the better is the overall match between the data and the model output. However, achieving a good match is only a necessary, but not sufficient condition for a successful inversion. Strong parameter correlations may lead to an ill-posed inverse problem which results in large estimation uncertainties [*Finsterle and Persoff*, 1996]. Therefore, it is imperative to analyze the covariance matrix of the estimated parameters, $\mathbf{C}_{pp}$, which contains the variances and correlation structure of the estimated parameter set. A linear approximation of $\mathbf{C}_{pp}$ is given by:

$$\mathbf{C}_{pp} = s_0^2 \left(\mathbf{J}^T \mathbf{C}_{zz}^{-1} \mathbf{J} \right)^{-1} \tag{10}$$

where $\mathbf{J}$ is the Jacobian matrix at the solution. Its elements are the sensitivity coefficients of the calculated system response with respect to the parameters:

$$J_{ij} = -\frac{\partial r_i}{\partial p_j} = \frac{\partial z_i}{\partial p_j} \tag{11}$$

If correlations among the parameters exist, the uncertainty of one parameter increases the uncertainty of the other parameters. In other words, the diagonal elements of matrix $\mathbf{C}_{pp}$ are the variances of the joint probability density function. While they take into account the effect from all the concurrently estimated parameters, they are usually too optimistic because of the assumption that all the remaining input parameters of the model are exactly known. Furthermore, they do not capture the uncertainty in the conceptual model usually leading to systematic errors in the estimates greater than the uncertainty from the random measurement errors.

To analyze the overall parameter correlation, we define $\sigma_p{}^*$ as the marginal standard deviation of a single parameter, i.e., the uncertainty of a parameter assuming that all other parameters are fixed, and σ_p as the joint standard deviation, i.e., the square-root of the diagonal element of $\mathbf{C}_{pp}$. We propose the ratio $\sigma_p{}^*/\sigma_p$ as a measure of overall parameter correlation. A value close to one signifies an independent estimate, whereas small values

indicate a loss of parameter identifiability due to its correlation to other uncertain parameters. Finally, we evaluate the trace of the covariance matrix as a measure of overall estimation uncertainty.

Results and Discussion

The results of the four inversions performed are summarized in Table 2. The s_0^2-values indicate that the data from the single-step experiment are better matched than those from the multi-step experiment. However, the overall estimation uncertainty, as measured by the trace of $\mathbf{C}_{pp}$, is lower for the multi-step experiment. This is only possible if the multi-step experiment yields more independent parameter estimates than the single-step experiment. In fact, the multi-step experiment yields consistently higher ratios between the marginal, σ_p^*, and joint standard deviation, σ_p, indicating lower parameter correlations. The stepwise change of suction pressures at the extraction cylinder effectively decouples the parameters due to the change in relative sensitivities. We consider this outcome to be a strong advantage of the multi-step over the single-step experiment. Systematic and random errors in the data and the model become apparent and have less impact on the estimates.

Table 2. Summary of results from the inversion of single-step and multi-step experiment using the BCB and VGM model.

Model	Parameter	Single-Step Experiment			Multi-Step Experiment		
		Estimate	σ	σ^*/σ	Estimate	σ	σ^*/σ
BCB	$\log(k_{abs})$	-12.80	0.06	0.06	-13.11	0.06	0.32
	λ	0.092	0.002	0.15	0.095	0.003	0.35
	$\log(p_e)$	2.91	0.04	0.05	2.97	0.03	0.30
	s_0^2	0.31	-	-	1.55	-	-
	$\mathrm{trace}(\mathbf{C}_{pp})$	0.006	-	-	0.004	-	-
VGM	$\log(k_{abs})$	-10.83	0.09	0.05	-11.47	0.09	0.18
	n	1.094	0.002	0.13	1.111	0.004	0.22
	$\log(1/\alpha)$	2.95	0.04	0.06	3.15	0.04	0.23
	s_0^2	0.42	-	-	1.33	-	-
	$\mathrm{trace}(\mathbf{C}_{pp})$	0.010	-	-	0.010	-	-

Table 3. Matrix of Direct and Total Parameter Correlations From the Inversion of the Multi-Step Experiment using the BCB Model.

	$\log(k_{abs})$	λ	$\log(p_e)$
$\log(k_{abs})$	3.29E-3	-0.92	-0.94
λ	-0.35	6.38E-6	0.93
$\log(p_e)$	-0.60	0.49	1.11E-3

Diagonal:	Variances of estimated parameters
Upper triangular matrix:	Correlation coefficients
Lower triangular matrix:	Matrix of direct correlations

The estimation uncertainty and correlation structure of the three parameters are shown in Table 3. The lower triangular matrix contains the correlation coefficients assuming that only pairs of parameters are estimated. These direct parameter correlations can be qualitatively assessed as follows. Since a reduction of λ leads to a reduced relative permeability, the absolute permeability has to be increased to approximately maintain the measured outflow. This explains the negative correlation coefficient between $\log(k_{abs})$ and λ. Similarly, the observed capillary pressure is achieved if permeability is increased and p_e is decreased, and vice versa, again explaining the negative sign of the correlation coefficient. Finally, an increase in p_e, which leads to stronger capillary pressures for a given saturation, can be partly compensated by an increase in the pore size distribution index λ. The latter reduces capillary pressures, and leads to a positive correlation coefficient. The upper triangular matrix in Table 3 contains the correlation coefficients as obtained by concurrently estimating all three parameters. They include contributions from indirect correlations which are difficult to interpret. We observe that the negative correlation between $\log(k_{abs})$ and λ is accentuated by the indirect correlations between $\log(k_{abs})$ and $\log(p_e)$, and $\log(p_e)$ and λ. Note that not the direct correlations, but the total correlations of the upper triangular matrix determine the uncertainty of the estimated parameters. The absolute values of the correlation coefficients are high, but not unreasonable as confirmed by the low standard deviations of the estimated parameters.

Figures 7 and 8 show the match obtained with the BCB model for the single-step and multi-step desaturation experiments, and also shown is the pressure applied at the extraction cylinder. The data from the single-step experiment are well matched by the model, whereas some systematic deviations can be seen between the model and the early-time flow data as well as the late-time pressure data for the multi-step experiment. If the actual pore space geometry is slightly different from the uni-modal distribution underlying the BCB model, this leads to deviations in the amount of liquid extracted at early times [*Durner*, 1994]. Similarly, the idealized shape of the capillary pressure curve near residual liquid saturation with its

asymptotic behavior may explain the deviations in the late-time pressure response. Hysteretic effects could also be important while the water is redistributed within the sample after an increase of the applied suction pressure.

It is interesting to note that the BCB and VGM models are equally suited to match the observed data. However, there is a large discrepancy in the estimated permeability values. The VGM model requires a significantly larger absolute permeability to match the outflow data. Estimating a high permeability seems necessary to compensate for the sharp decline of the relative permeability curve near full saturation. Figure 9 shows the BCB and VGM relative permeability functions for the respective best estimate parameter set. Despite the large gap between the two curves, the resulting effective permeabilities, which determine the transient flow behavior, are very similar. To illustrate this, we have multiplied the VGM relative permeabilities with the ratio of the estimated absolute permeabilities, yielding almost identical effective permeabilities over the range of saturations encountered during the experiment.

Figure 10 shows that both the BCB and VGM models with the estimated parameter values lead to very similar capillary pressure curves. Furthermore, the approximate relations $1/\alpha \approx p_e$ and $n \approx \lambda + 1$ [Morel-Seytoux, 1996] seem to hold in this case (see Table 2). Also shown in Figure 10 are the data points taken from the observed data. The symbols are the average saturations calculated from the cumulative outflow data and the corresponding capillary pressures from the tensiometer. This data set could be used to directly match a VGM or BCB model, i.e., without performing a flow simulation. However, a small error is introduced by making the equilibrium assumption. In inverse modeling, transient effects are automatically taken into account, shifting the resulting capillary pressure curve to the right as expected.

The advantage of concurrently estimating absolute permeability and unsaturated hydraulic properties from a transient desaturation experiment using inverse modeling with ITOUGH2 has been demonstrated. If the absolute permeability were measured independently, and the VGM model were chosen to match capillary pressure data from a traditional desaturation experiment assuming equilibrium, the predictions made with the resulting parameter set would be wrong due to an underestimation of effective permeability by almost two orders of magnitude. The transient experiments analyzed here provide a means to obtain a consistent parameter set, improving the reliability of subsequent model predictions. Moreover, with an independent permeability estimate, it is possible to can discriminate between the BCB and VGM model. In our case, saturated permeability measurements on the same core indicate that the high permeability obtained with the VGM model is not reasonable, making the parameter from the BCB model the preferred solution.
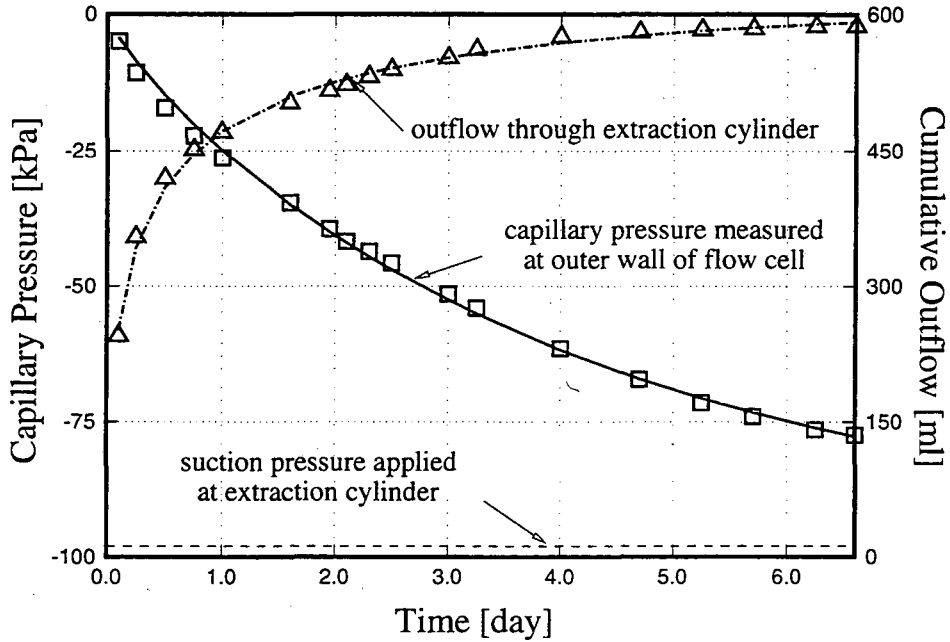
Figure 7. Comparison between observed (symbols) and simulated (lines) system response for the single-step radial flow experiment.
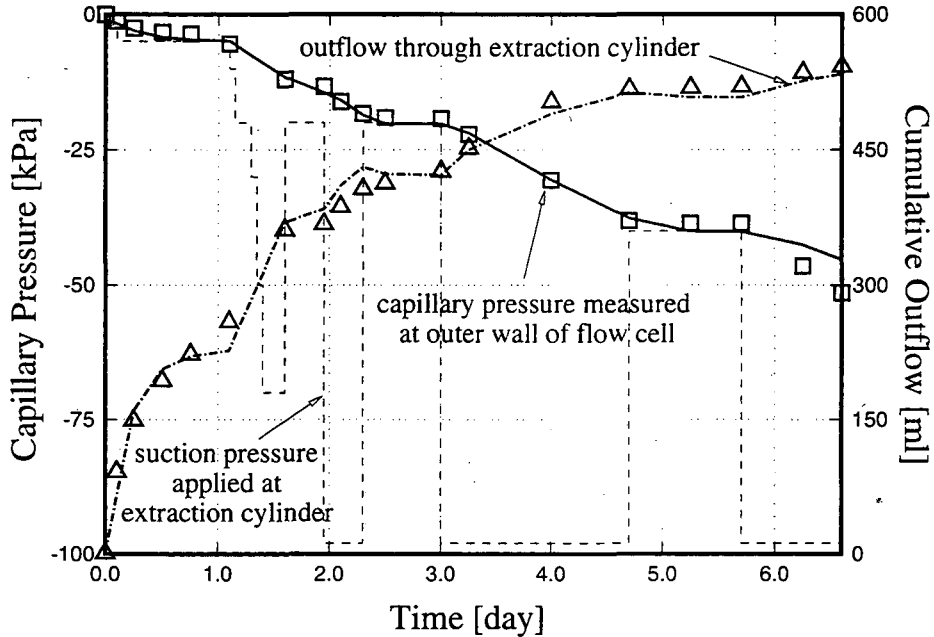
Figure 8. Comparison between observed (symbols) and simulated (lines) system response for the multi-step radial flow experiment. The prescribed suction pressure at the extraction cylinder is shown as a dashed line.
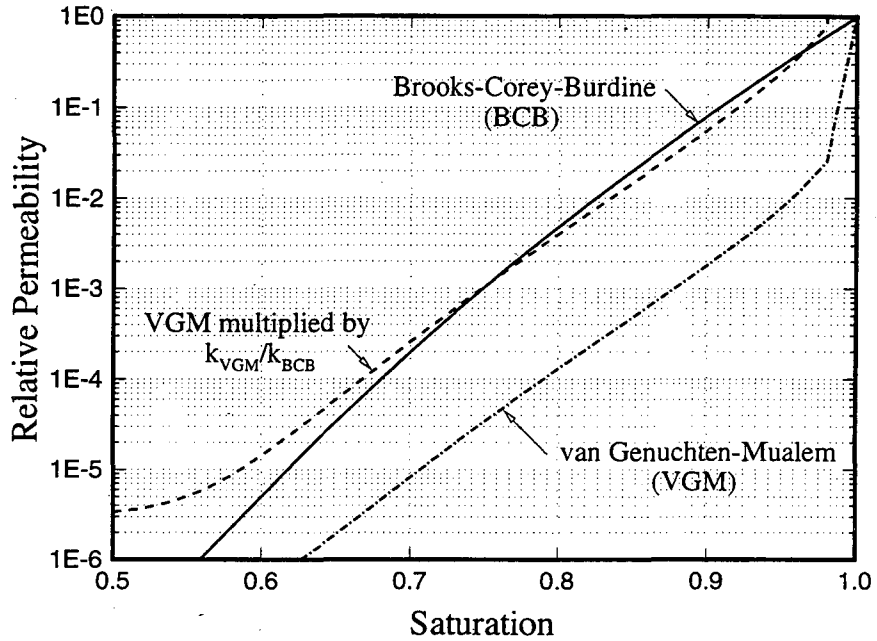
Figure 9. Relative permeability function derived by inverse modeling for the Brooks-Corey-Burdine and the van Genuchten-Mualem model.
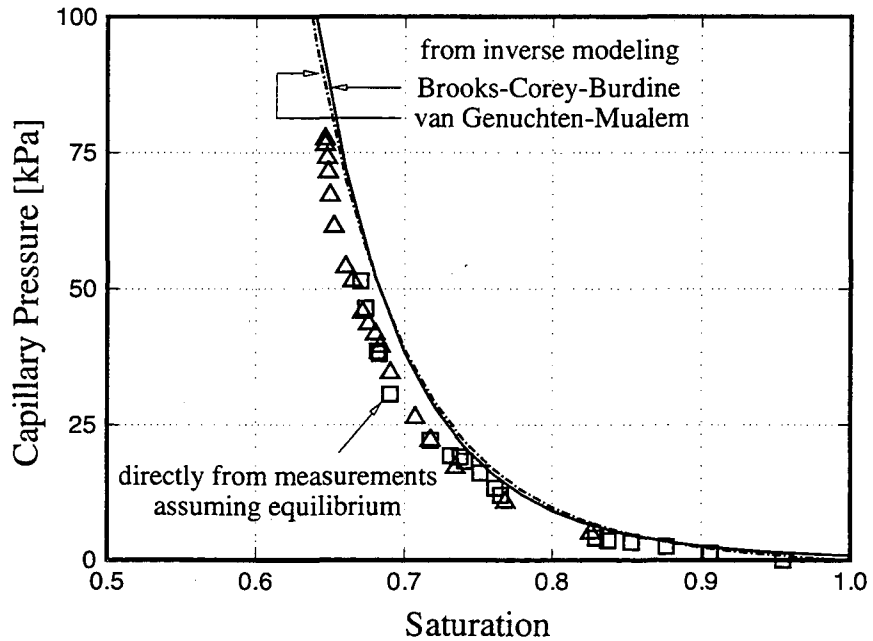
Figure 10. Capillary pressure function directly inferred from the data assuming equilibrium, and by inverse modeling using the BCB and VGM models, which takes into account transient effects.

Summary and Concluding Remarks

We have performed single-step and multi-step radial desaturation experiments on soil samples, and analyzed the transient flow and pressure data using inverse modeling. The suitability of the proposed experimental design for the determination of unsaturated hydraulic properties has been assessed. Recall that experimental design includes the setup of the apparatus, the selection of observation types and measuring points, and the regime of applied suction pressures.

The following conclusions can be drawn. The radial flow experiment provides sensitive data for the simultaneous determination of absolute permeability and the parameters of the relative permeability and capillary pressure functions. All parameters are determined with a single experiment performed on a single core. Installation of the tensiometer near the outer wall of the flow cell is a (slightly) sub-optimal, but robust configuration to be preferred over alternative designs. Collecting transient flow data from a multi-step experiment provides additional information on each pressure step needed to constrain the effective permeability governing unsaturated flow.

In many cases, applying conventional curve fitting procedures to capillary pressure data collected under equilibrium conditions does not allow one to distinguish between alternative conceptual models such as the Brooks-Corey-Burdine or van Genuchten-Mualem model. As a consequence, predictions made with the resulting parameter set may be erroneous if the wrong model is chosen. It is therefore important to actually simulate a transient experiment, capturing the relevant processes governing unsaturated flow, as opposed to inferring effective permeabilities from a pore size distribution model only.

Inverse modeling provides the necessary flexibility to analyze these data which contain significantly more information about the system to be modeled. In our case, not only information about the relationship between saturation and capillary pressure was obtained, but also regarding effective permeability. Given an independent estimate of absolute permeability, it was possible to discard the van Genuchten-Mualem functions as a model for the investigated soil sample. If an independent permeability measurement is unavailable, the value concurrently estimated by inverse modeling partly compensates for the error in the model, making the subsequent predictions more accurate.

The proposed experimental design and analysis procedure will be used in the future to investigate additional effects such as temperature, entrapped air, anisotropy, and hysteresis.

References

Beck, J. V., and K. J. Arnold, *Parameter estimation in engineering and* science, John Wiley & Sons, New York, 1977.

Brooks, R. H., and A. T. Corey, Hydraulic properties of porous media, Hydrol. Pap., Colorado State Univ., Fort Collins, 3, 1-27, 1964.

Burdine, N. T., Relative permeability calculations from pore size distribution data, *Petr. Trans. Am. Inst. Mining Eng.*, 198, 71-78, 1953.

Clausnitzer, V., J. W. Hopmans, and D. R. Nielson, 1992, Simultaneous scaling of soil water retention and hydraulic conductivity curves, *Water Resour. Res., 28* (1), 19-31.

Durner, W., Hydraulic conductivity estimation for soils with heterogeneous pore structure, *Water Resour. Res.*, 30(2), 211-223, 1994.

Dzekunov, N. E., I. E. Zhernov, and B. A. Faybishenko, 1987, Thermodynamic methods of investigating the water regime in the vadose zone, Moscow, Nedra, 177.

Faybishenko, B. A., 1986, Water-salt regime of soils under irrigation, Moscow, Agropromizdat, 314 p.

Finsterle, S., ITOUGH2 command reference, Version 3.1, Report LBL-40041, Lawrence Berkeley National Laboratory, Berkeley, Calif., 1997.

Finsterle, S., and P. Persoff, Determining permeability of tight rock samples using inverse modeling, paper submitted to *Water Resour. Res.*, Report LBNL-39296, Lawrence Berkeley National Laboratory, Berkeley, CA, 1996.

Finsterle, S. , and K. Pruess, Solving the Estimation-Identification Problem in Two-Phase Flow Modeling, *Water Resour. Res.*, 31(4), 913-924, 1995.

Finsterle, S., and K. Pruess, Design and analysis of a well test for determining two-phase hydraulic properties, paper submitted to *Water Resour. Res.*, Report LBNL-39620 Lawrence Berkeley National Laboratory, Berkeley, CA, 1996.

Gardner, W. R., Calculation of capillary conductivity from pressure plate outflow data, *Soil Sci. Soc. Am. Proc.*, 20, 317-320, 1956.

Knopman, D. S., and C. I. Voss, Behavior of sensitivities in the advection-dispersion equation: Implications for parameter estimation and sampling design, *Water Resour. Res.*, 24(2), 225-238, 1988.

Knopman, D. S., and C. I. Voss, Multiobjective sampling design for parameter estimation and model discrimination in groundwater solute transport, *Water Resour. Res.*, *25*(10), 2245-2258, 1989.

Knopman, D. S., C. I. Voss, and S. P. Garabedian, Sampling design for groundwater solute transport: Tests of methods and analysis of Cape Cod tracer test, *Water Resour. Res.*, *27*(5), 925-949, 1991.

Kool, J. B., J. C. Parker, and M. Th. van Genuchten, Determining soil hydraulic properties from one-step outflow experiments by parameter estimation: I. Theory and numerical studies, *Soil Sci. Soc. Am.*, *49*, 1348-1354, 1985.

Luckner, L., M. Th., van Genuchten, and D.R. Nielsen, 1989, A consistent set of parametric models for the two-phase flow of immiscible fluids in the subsurface, *Water Resour. Res.*, *25* (10), 2187-2193.

Luthin, J. N. (Ed.), *Drainage in agricultural lands*, Am. Soc. of Agron., Madison, Wis., 1957.

Morel-Seytoux, H. J., P. D. Meyer, M. Nachabe, J. Touma, M. Th. van Genuchten, and R. J. Lenhard, Parameter equivalence for the Brooks-Corey and van Genuchten soil characteristics: Preserving the effective capillary drive, *Water Resour. Res.*, 32(5), 1251-1258, 1996.

Mualem, Y., A new model for predicting the hydraulic conductivity of unsaturated porous media, *Water Resour. Res.*, *12*(3), 513-522, 1976.

Perfect, E., N. B. McLaughlin, B. D. Kay, and G. C. Topp, An improved fractal equation for the soil water retention curve, *Water Resour. Res.*, 32(2), 281-287, 1996.

Pruess, K., TOUGH2 - a general-purpose numerical simulator for multiphase fluid and heat flow, Report LBL-29400, Lawrence Berkeley National Laboratory, Berkeley, Calif., 1991.

Rawls and Brakensiek, Estimation of soil water retention and hydraulic properties, in H. J. Morel-Seytoux (ed.), *Unsaturated Flow in Hydrologic Modeling, Theory and Practice*, 275-300, Kluwer Academic Publishers, 1989.

Salehzadeh, A., and A. H. Demond, Apparatus for the rapid automated measurement of unsaturated soil transport properties, *Water Resour. Res.*, *30*(10), 2679-2690, 1994.

Saxton, K. E., W. J. Rawls, J. S. Romberger, and R. I. Papendick, Estimating generalized soil-water characteristics from texture, *Soil Sci. Soc. Am. J.*, *50*, 1031-1036, 1986.

Simunek, J., and M. Th. van Genuchten, Estimating unsaturated soil hydraulic properties from tension disc infiltrometer data by numerical inversion, *Water Resour. Res.*, *32*(9), 2683-2696, 1996.

Steinberg, D. M., and W. G. Hunter, Experimental design: Review and comment, *Technometrics*, *28*, 71-97, 1984.

Sun, N., and W. Yeh, Coupled inverse problems in groundwater modeling, 2. Identifiability and experimental design, *Water Resour. Res.*, *26*(2), 2527-2540, 1990.

van Genuchten, M. Th., A closed-form equation for predicting the hydraulic conductivity of unsaturated soils, *Soil Sci. Soc. Am. J.*, *44*, 892-898, 1980.